Article

Process Development and Scale-up of the Continuous Flow Nitration of Trifluoromethoxybenzene

Zhenghui Wen,[†,‡] Fengjun Jiao,[†] Mei Yang,[†] Shuainan Zhao,[†,‡] Feng Zhou,[†,‡] and Guangwen Chen*,[†]

[†]Dalian National Laboratory for Clean Energy, Dalian Institute of Chemical Physics, Chinese Academy of Sciences, Dalian 116023, China

[‡]University of Chinese Academy of Sciences, Beijing 100049, China

S Supporting Information

ABSTRACT: In this work, continuous flow nitration of trifluoromethoxybenzene (TFMB) was conducted in a microchannel reactor. The effects of process parameters, including temperature, residence time, sulfuric acid strength, flow rate, and reactor structure, were systemically investigated. It was found that the aforementioned process parameters had significant effect on TFMB conversion, while the product selectivity was merely sensitive to the reaction temperature. On the basis of the results of process parameter optimization, a scale-up strategy combining microreactor with distributed packed tubular reactor was presented. Consequently, excellent performance was achieved in the combined reactor with a kilogram-scale production.

1. INTRODUCTION

Trifluoromethoxy aniline is an important intermediate involved in the synthesis of a wide range of fine chemicals, for example, pesticides,[1] pharmaceuticals,[2] and liquid crystal materials.[3] It is generally produced via the nitration of trifluoromethoxybenzene (TFMB) with mixed acid followed by reduction of nitration products. Generally, the nitration reactions are often difficult to control due to its extremely fast rate and highly exothermic nature, with the reaction heat ranging from −73 to −253 kJ·mol^{-1}.[4] Due to the inefficient transport properties of stirred batch reactors, the nitration of TFMB (Figure 1) is always operated at very low reaction temperature (263 K), reactant concentration, and adding rate of mixed acid (28 h) to achieve a mild condition and inhibit the formation of undesired products (m-NB and DNB). Apparently, the nitration of TFMB in stirred batch reactor is a time-consuming and low-efficiency process.[5] Therefore, it is very important and urgent to develop a new strategy based on process intensification technology to improve the productivity and process safety.

As a typical process intensification technology, the microreactor has opened up new horizons both in academia and industry. Owing to the characteristic dimension of submillimeter, the microreactor possesses a large surface-to-volume ratio, enhanced mass and heat transfer rate, precise control over reaction parameters, high integration, and inherent process safety,[6] which hold great promise for very fast and highly exothermic reactions. The microreactor has been applied to intensify the nitration reaction recently.[7] Yu et al.[7d] proposed a continuous flow nitration process to produce 2,5-difluoronitrobenzene, and a 98% yield with an output being 6.25 kg/h was realized. In addition, the shorter residence time (2.3 min) in microreactor meant higher efficiency in comparison to the batch reactor (>1 h). Brocklehurst et al.[8] used a commercially available continuous flow reactor to perform the challenging nitration of 2-amino-4-bromobenzoic acid methyl ester with a 84% yield and 70 g/h production rate. Noticeably, no byproduct was obtained, which greatly simplified the process

of the workup. Apart from those substantial advantages presented above, with the numbering-up strategy, the small scaling effect of microreactor makes the laboratory results easier to industrialize.[9] Gage et al.[10] reported the continuous flow nitration of 5-bromo-2-amino-4-methylpyridine from kilogram scale in the laboratory to 100 kg scale in the plant with a 99.7% purity and 50% yield.

In this study, we performed the continuous flow nitration of TFMB in the microreactor system. Considering that the next step of the nitration of TFMB was the reduction of the mononitration product, it was difficult to separate isomers of trifluoromethoxybenzenamine. Therefore, the selectivity of m-NB and DNB should be controlled as low as possible to cut the cost of the separation. The objective was to minimize the byproduct selectivity (m-NB < 0.1%, DNB < 1.5%) without decline of the product yield, which could bring significant economic benefits in saving costs of downstream separation and products purification. First, the effects of process parameters on the conversion of TFMB and product selectivity were investigated in detail. The best performance in terms of yield and selectivity was obtained by means of process optimization. Subsequently, on the basis of the results of process development, a scale-up strategy which combined a multichannel microreactor with a distributed packed tubular reactor was proposed, and kilogram-scale production was achieved in the combined reactor.

2. RESULTS AND DISCUSSION

2.1. Process Development. *2.1.1. Effect of the Reaction Temperature.* The reaction temperature plays a significant role in the process of nitration reaction. Given that aromatic nitration reaction is a typically heterogeneous reaction, temperature influences not only the mass transfer of organic compounds into the acid phase, but also the intrinsic reaction
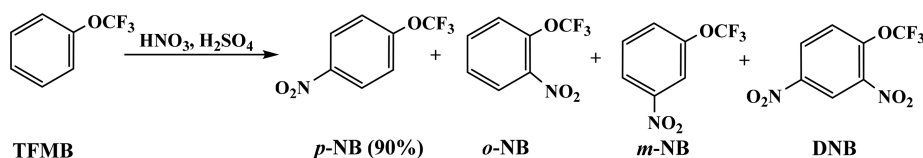
Figure 1. Nitration of TFMB with the *o*-NB and *p*-NB as the main products and *m*-NB and DNB as side products.
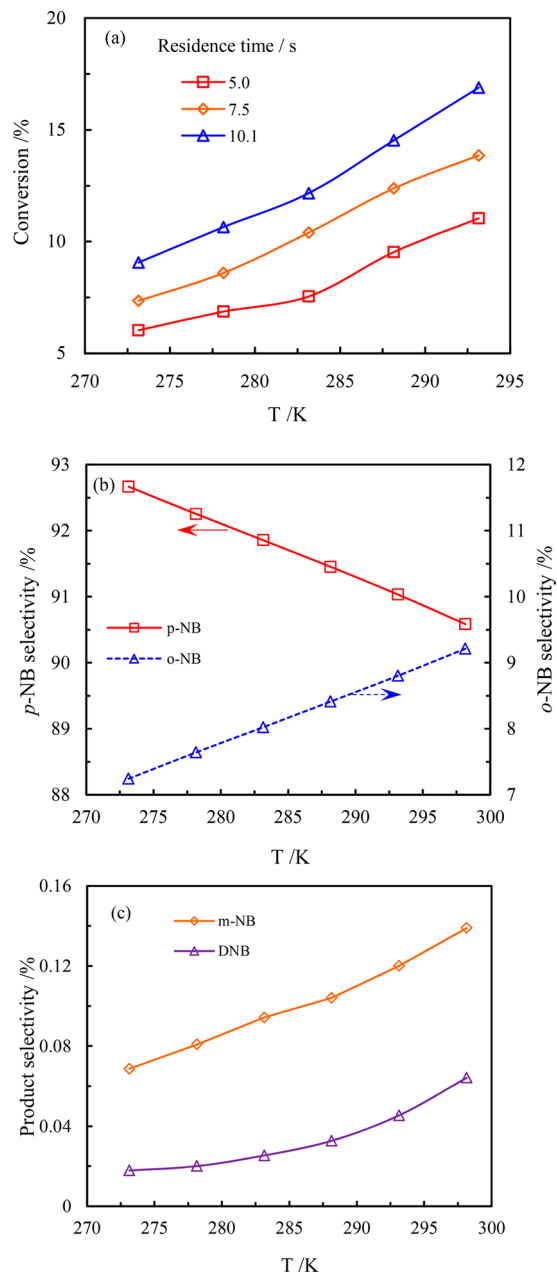

Figure 2. Effect of reaction temperature on the (a) conversion of TFMB and (b, c) product selectivity. Molar ratio of HNO_3 to H_2SO_4 (N/S) = 0.2, molar ratio of HNO_3 to TFMB (N/F) = 0.86, t = 5.0 s, sulfuric acid strength $[\varphi = w_s/(w_w + w_s)]$ = 89 wt %, Q_{or} = 0.5 mL·min^{-1}, Q_{aq} = 1.2 mL·min^{-1}.

Figure 3. Effect of residence time on the (a) conversion of TFMB and (b, c) product selectivity. N/S = 0.2, N/F = 0.86, T = 278 K, Q_{or} = 0.5 mL·min^{-1}, Q_{aq} = 1.2 mL·min^{-1}.

rate. Figure 2 shows the effect of reaction temperature on the conversion of TFMB and product selectivities at different residence times. The main product is *p*-NB that counts more than 90% of the products due to the small rotation barrier of the OCF_3 group.[1] The product selectivity follows the order *p*-NB > *o*-NB > *m*-NB. With the increase of reaction temperature,
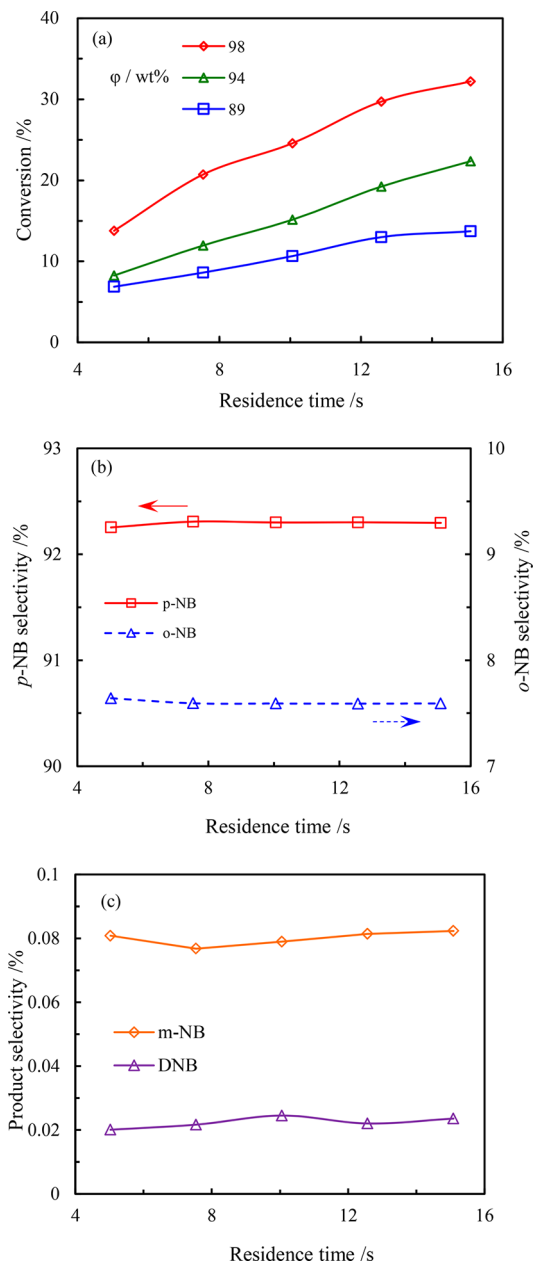
the selectivity of *p*-NB decreases, while those of *m*-NB and *o*-NB increase. According to our previous research, it was due to that the activation energies of ortho- and meta-nitrations are larger than that of para-nitration. It is reasonable that attacking the ortho-position and meta-position of the aromatic ring by NO_2^+ are more difficult, considering the rotational barrier in TFMB molecules. Therefore, higher temperature is propitious to promote the ortho- and meta-nitrations. As we all know, the
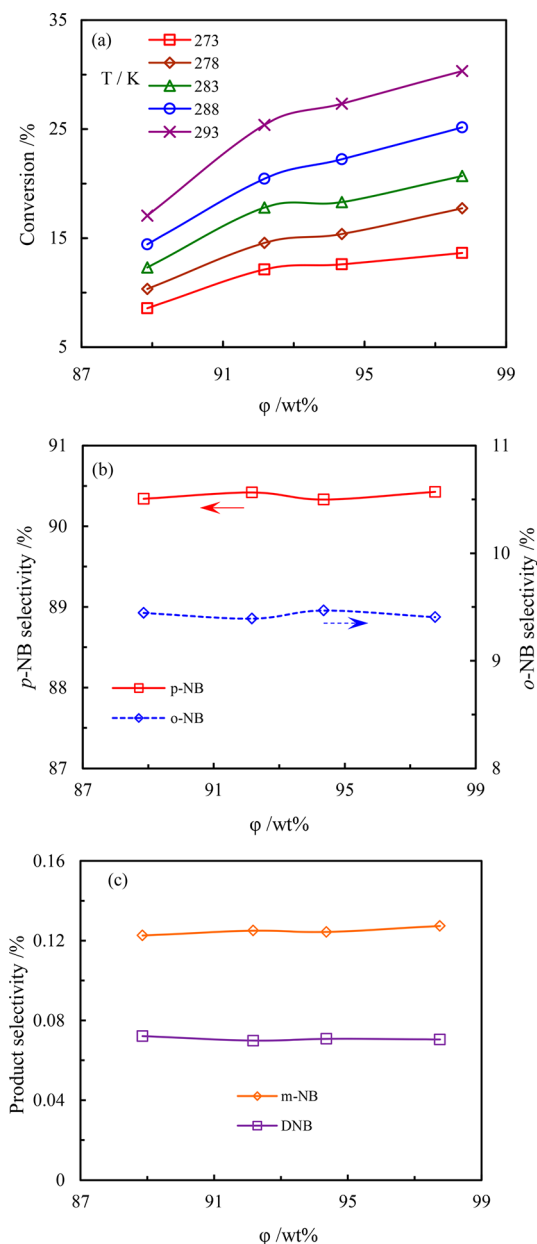
Figure 4. Effect of sulfuric acid strength on the (a) conversion of TFMB and (b, c) product selectivity. N/S = 0.2, t = 7.5 s, T = 293 K, Q_{or} = 0.5 mL·min^{-1}, Q_{aq} = 1.2 mL·min^{-1}.

Figure 5. Effect of the molar ratio of HNO$_3$/TFMB on the (a) conversion of TFMB and (b, c) product selectivity. N/S = 0.2, t = 7.5 s, T = 293 K, Q_{or} = 0.5 mL·min^{-1}, Q_{aq} = 1.2 mL·min^{-1}.

nitro group is a deactivating group, so it would be harder for NO$_2^+$ to attack the mononitration products. Therefore, the higher reaction temperature would be conductive to the DNB formation.

2.1.2. Effect of Residence Time. Residence time is another important parameter which affects the reagent conversion and product selectivity. Too short of a residence time may lead to a low conversion of reagent, while a long residence time would let reagent pointlessly flow inside the microreactor, and some intermediates may convert to side product, decreasing the selectivity of the main product.[12] Similarly, excessive nitration may occur during a prolonged residence time and produce undesired products in nitration reaction. Therefore, the residence time should be precisely controlled to obtain the highest yield of desired product. In this section, the residence time of the experiment was changed by varying the length of
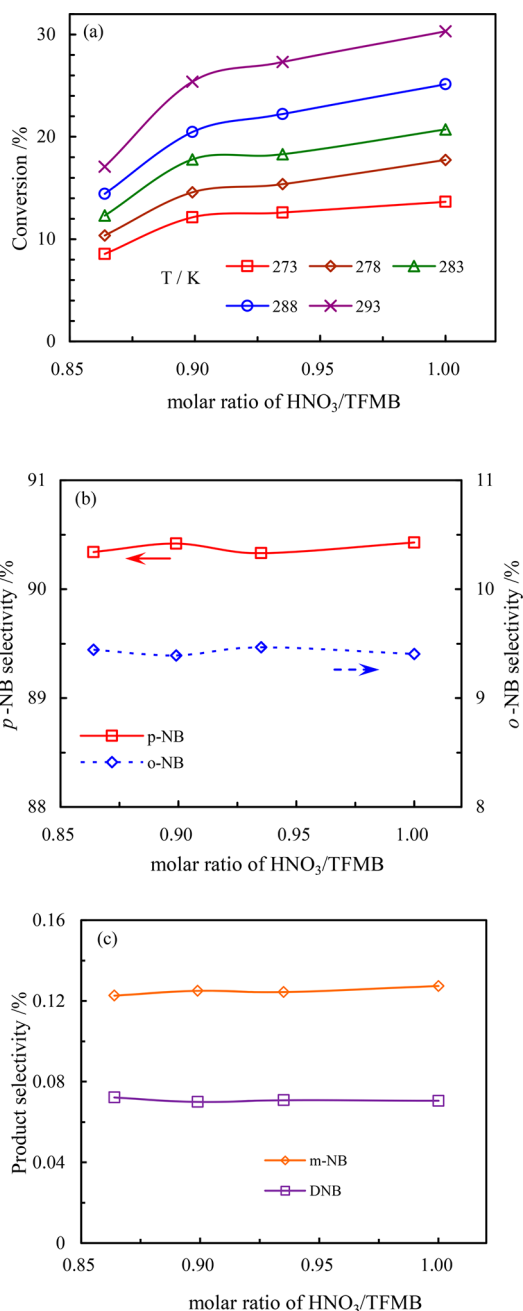
microchannel reactor. The effect of residence time was investigated under the reaction conditions of N/S = 0.2, N/F = 0.86, T = 278 K, Q_{or} = 0.5 mL·min^{-1}, Q_{aq} = 1.2 mL·min^{-1}. Figure 3 demonstrates the effect of residence time on the conversion of TFMB and product selectivity. It is observed that a longer residence time will result in a higher conversion of TFMB, especially with mixed acid of a higher sulfuric acid strength. Nevertheless, the product selectivity nearly remains unchanged with the increasing residence time during the experiments, which may due to the fact that the residence time is not long enough to reflect its influence on the product selectivity.

2.1.3. Effect of Sulfuric Acid Strength. It is widely accepted that, when a nitration reaction is carried out with the mixed
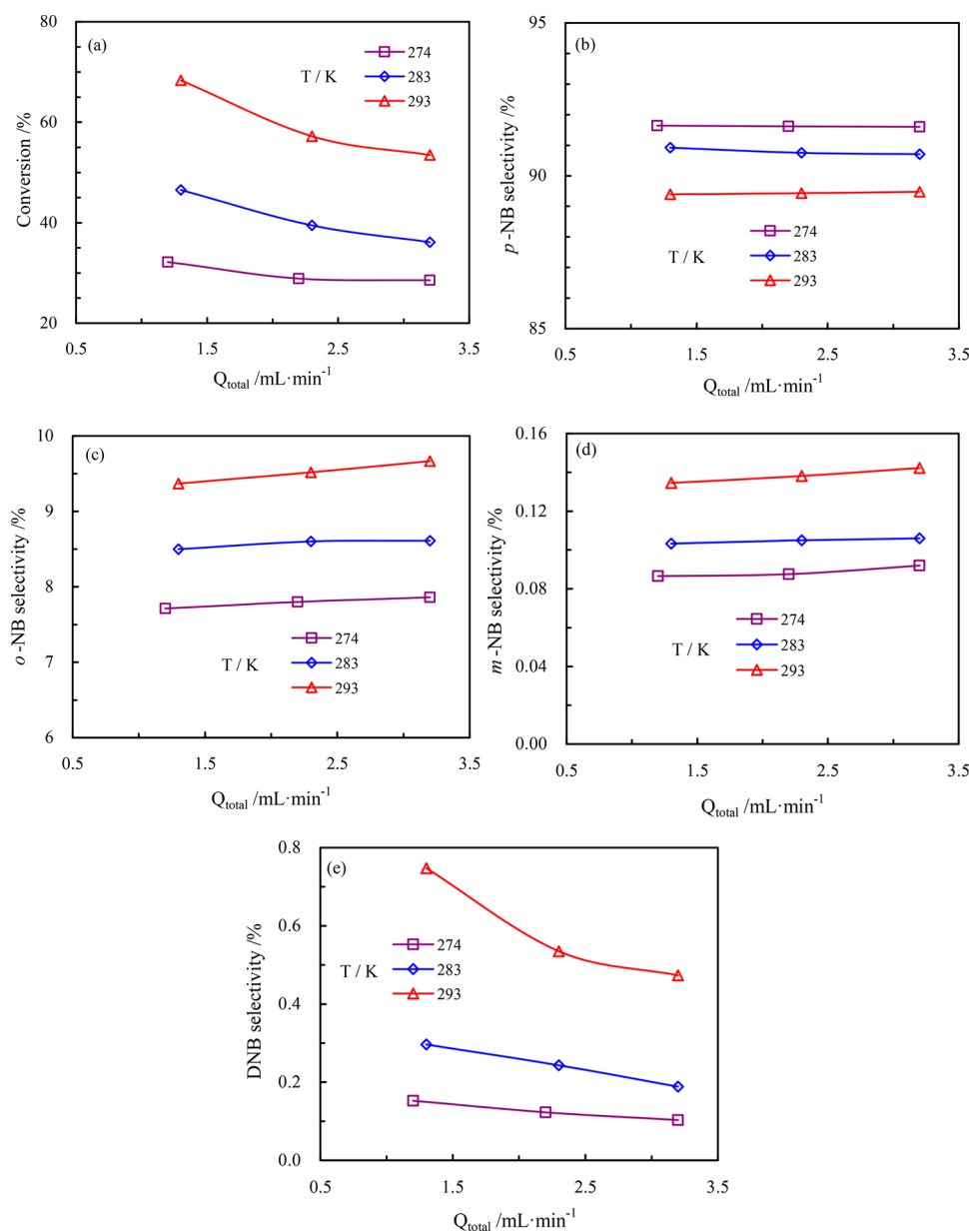
Figure 6. Effect of flow rate on the (a) conversion of TFMB and (b, c, d, e) product selectivity. N/S = 0.25, N/F = 1.1, φ = 97 wt %.

acid, sulfuric acid acts as a catalyst, which protonates nitric acid and generates NO_2^+ ions.[13] Therefore, to obtain the optimized process parameters, the effect of sulfuric acid strength on the conversion of TFMB and product selectivity should be studied in detail. As shown in Figure 4a, conversion of TFMB increases with increasing sulfuric acid strength. Considering that nitration reactions with mixed acid generally are heterogeneous, higher sulfuric acid strength not only promotes the generation of NO_2^+ ions but also increases the solubility and mass transfer rate of TFMB in acid phase.[14] Both of these enhance the nitration rate and then result in a high conversion of TFMB. As displayed in Figure 4b and c, the product selectivities are nearly not affected with the increase in sulfuric acid strength. This is due to the fact that the reactions of para-, ortho-, and meta-nitrations are parallel and the reaction improvements caused by increasing sulfuric acid strength are similar. Similarly, the unchanged selectivity of DNB can also be explained by that.

2.1.4. Effect of the Molar Ratio of $HNO_3/TFMB$. As we all know, an appropriate molar ratio of reaction reagents can promote the conversion of reagent and enhance the selectivity of desired product. In addition, it can also simplify the workup procedure and reduce the waste. The effect of molar ratio of $HNO_3/TFMB$ on the conversion of TFMB and product selectivity is presented in Figure 5. As shown in Figure 5, it is found that the conversion of TFMB increases with increasing molar ratio, while the product selectivities remains unchanged. This is attributed to more NO_2^+ ions generated for nitration. As for the unchanged product selectivities, this is due to the fact that the mononitration reactions are parallel and the reaction orders are identical. Besides, the residence times in the experiments of this section is not long enough for the complete conversion of reactant TFMB, which decreases the occurrence of side reaction to some extent.

2.1.5. Effect of Flow Rate. The flow rate is a vital parameter in conducting nitration reaction. In this section, the length of the microchannel was kept constant, which meant that the residence time decreased with the increasing flow rate. Figure 6 demonstrates the effect of flow rate on the conversion of
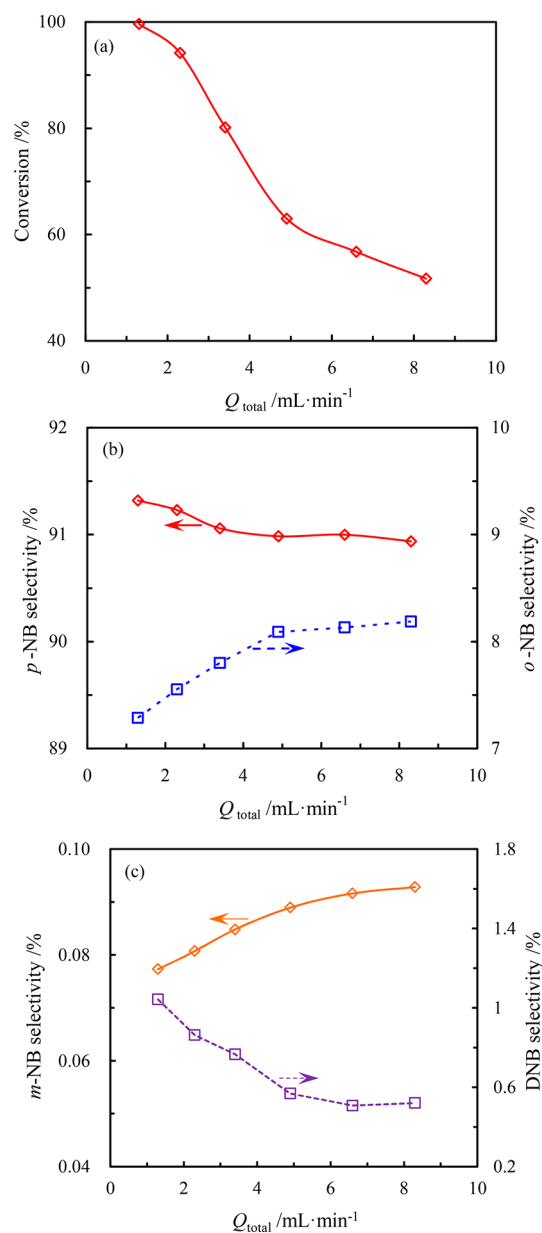
Figure 7. Effect of flow rate on the (a) conversion of TFMB and (b, c) product selectivity in a packed microchannel system. N/S = 0.25, N/F = 1.1, φ = 97 wt %, T = 273 K.

TFMB and product selectivity. It can be seen from Figure 6a that the conversion of TFMB decreases slightly with the increase in flow rate. On one hand, as the flow rate increased from 1.3 to 3.2 mL·min⁻¹, the residence time decreased from 8.0 to 3.2 s, which leaded a lower conversion of TFMB. On the other hand, higher flow rate will also enhance mass transfer rate,[15] which benefited TFMB nitration. Evidently, increasing total flow rate exerted an opposite effect on the conversion of TFMB. As a result, TFMB conversion was determined by the integrated outcome of these two changes. It also implicates that these nitration processes are still limited by mass transfer in the microchemical system. As shown in Figure 6b−d, the product selectivities of mononitrations nearly remain unchanged with the increasing flow rate, which indicates that the performance of microreactor in heat transfer is excellent. It is obvious in Figure 6e that the selectivity of dinitration product decreases sharply with the increase in flow rate. A faster flow rate would

result in a better mixing effect, which can make the organic compound more evenly dispersed in the acid phase. Besides, a faster flow rate would also decrease the residence time. Therefore, a faster flow rate could reduce the occurrence of dinitration.

2.1.6. Effect of Reactor Structure. Considering that the nitration processes were limited by the mass transfer in microchannel systems, the method of packing microparticles (micro packed-bed reactor) was taken up to intensify mass transfer process between the mixed acid and compound TFMB in microchannel system. In our previous work, it was found that better mixing and reaction performance could be obtained in the packed microchannel system because of its excellent mass transfer performance.[7c,16] In this section, the reaction system consisted of a microchannel reactor (length 0.1 m, inner diameter 0.6 mm) and a packed tubular reactor (length 0.3 m, inner diameter 6 mm). The quartz sand microparticles with an average size of 710 μm were packed in the tubular reactor at a porosity of 0.39. It is observed from Figure 7a that TFMB is totally converted at the low flow rate and then the conversion decreases directly with the increasing flow rate. Given such a low volume of the microreactor system, multiply increasing flow rates lead to a shorter residence time which is not enough for the full nitration of TFMB. The effect of the flow rate on product selectivities in a packed microchannel system are presented in Figure 7b, c, which are similar to the results mentioned in former section. What is different is that the variation of the product selectivities in this section is larger than that of former section, which also indicates that packing microparticles poses a challenge to the heat transfer in microchannel reactor. To take advantage of the enhanced mass transfer brought by the packed microparticles, several methods are set up to deal with the heat transfer problem in packed microchannel system during the scale up experiments, such as distributing the released heat, changing the size of packed microparticles, and reducing the reaction temperature.

2.2. Scale-up of the TFMB Nitration. As stated above, a broad range of reaction parameters for trifluoromethoxybenzene nitration process were investigated. The highest conversion (99.6%) was achieved in the microchannel coupled with packed tubular reactor system under the reaction conditions of N/S = 0.25, N/F = 1.1, φ = 97 wt %, T = 273 K, Q_{or} = 0.4 mL·min⁻¹, and Q_{aq} = 0.9 mL·min⁻¹, with the selectivity of o-NB, m-NB, p-NB, and DNB being 7.26%, 0.08%, 90.97%, and 1.04%, respectively. Encouraged by these results, the scale up of the nitration process of TFMB was further performed. As the conversion of TFMB could be dramatically increased by packing microparticles, the microreactor combined with the packed tubular reactor was chosen as the basic unit for the scaling up in this section, and several different strategies about packed tubular reactor were tested to obtain the best reaction performance.

2.2.1. Strategy A. The tubular reactor in Entry 1 consisted of four packed tubular reactors (stainless tube, length 1 × 675 mm + 3 × 900 mm, 12 mm o.d., 9 mm i.d.) with a porosity being 0.46. The size of the cylindrical quartz sand was 2 mm in diameter and 2 mm in length (Φ2 × 2). Figure 8 show the scaling-up experimental setup of the continuous flow nitration process. TFMB and mixed acid were pumped with the volume flow rate of 10 mL·min⁻¹ and 24.5 mL·min⁻¹, respectively. The mixture then flowed through the microreactor which was cooled by running water. After the quick mixing in microreactor
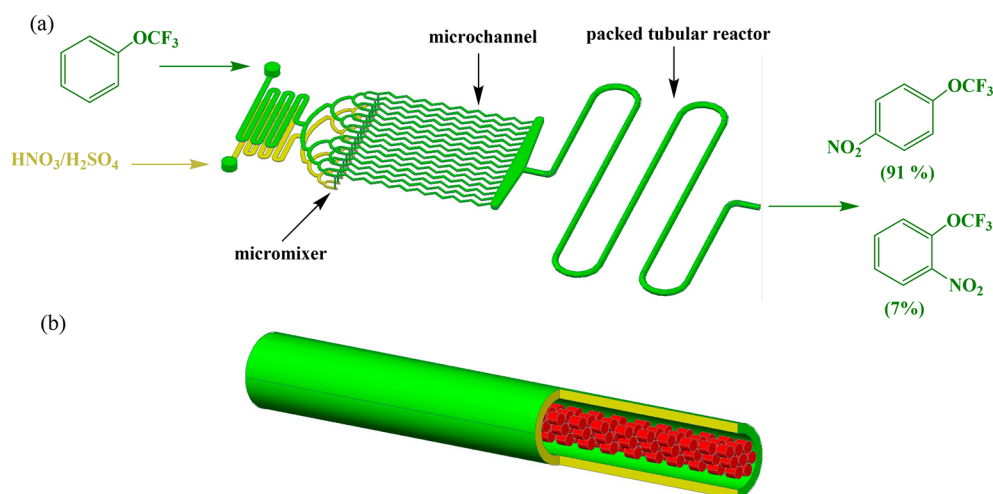
Figure 8. Schematic setup of strategy A for the scale up of the continuous flow TFMB nitration. (a) 3D model of setup of strategy A (b) cutaway picture of packed tubular reactor (red blocks represent packed microparticles).

Table 1. Screen of the Size of the Packed Particle on the Scale up of the Continuous Flow Nitration of TFMB

entry	GC mol %					
	TFMB	*p*-NB	*o*-NB	*m*-NB	DNB	conversion
1[a]	0.06	89.75	6.90	0.11	3.17	99.94
2[b]	0.00	91.32	6.69	0.08	1.90	100.0
3[c]	4.71	87.52	6.58	0.07	1.12	95.29

[a]Condition: All coilers were packed with the $\Phi2 \times 2$ cylindrical quartz sand. [b]The first coiler was packed with the $\Phi3 \times 3$ cylindrical quartz sand, while others remained the same. [c]The front half of coilers were packed with the $\Phi3 \times 3$ cylindrical quartz sand, while the another half remained the same.

(4.7 s), the mixture was delivered into the packed tubular reactor with a residence time being 2.8 min.

Following the workup of the mixture stream, the products were collected and analyzed by GC. As shown in Table 1, about 89.75% of *p*-NB, 6.9% of *o*-NB, and byproducts (0.11% of *m*-NB and 3.17% of DNB) were detected in the products. As mentioned above, the selectivities of byproducts were sensitive to temperature. The temperature rise of the flowing stream in the first coiler was found to be evidently high due to the fast nitration reaction in the first coiler, which was accompanied by much reaction heat. To avoid the sharp temperature rise, the reaction should proceed in a controlled manner. According to our previous work,[16] a smaller size of microparticles used in the packed tubular reactor leaded a higher effective interfacial area and better mixing efficiency. Hence, the size of the packed quartz sand in the first coiler was changed from $\Phi2 \times 2$ to $\Phi3$

$\times 3$, while other three coilers remained the same (Entry 2). It can be seen from Table 1 that the selectivities of the main product increased, while the byproducts decreased. However, the selectivity of DNB was still beyond our expectation. To further decrease the selectivity of byproduct DNB, another adjustment was adopted. The $\Phi3 \times 3$ quartz sand was still used to replace the $\Phi2 \times 2$ one (Entry 3). The selectivities of the byproducts decreased as we expected. Unfortunately, the conversion of TFMB also decreased (95.29%), which demonstrated that enlarging the size of the packed particles would slow down the reaction rate and further decrease the reaction heat. The key issue was pointed out to be distributing the reaction heat and controlling the reaction temperature without slowing down the reaction rate.

2.2.2. Strategy B. On the basis of the results of the strategy A, a new optimized strategy (Figure 9) was then proposed. Four tubular reactors with smaller diameter (stainless tube, 8 mm o.d., 6 mm i.d.) were used to take place the front half of the tubular reaction system, while the other half of reactor remained the same. A distributed design of the tubular reactors would be beneficial for the heat transfer of the reaction. And the packed $\Phi2 \times 2$ cylindrical quartz sand could also ensure the relatively quick reaction rate and that product TFMB was completely converted. As presented in Table 2, the optimal conditions were achieved by flowing TFMB and mixed acid [solution of fuming nitric acid in concentrated sulfuric acid (1:4)] at the rate of 10 mL·min^{-1} and 24.2 mL·min^{-1} (total residence time being 2.4 min) and controlling the reaction temperature below −2 °C. 91.08% of *p*-NB, 7.05% of *o*-NB, and only trace of *m*-NB (0.08%) and DNB (1.34%) were obtained,
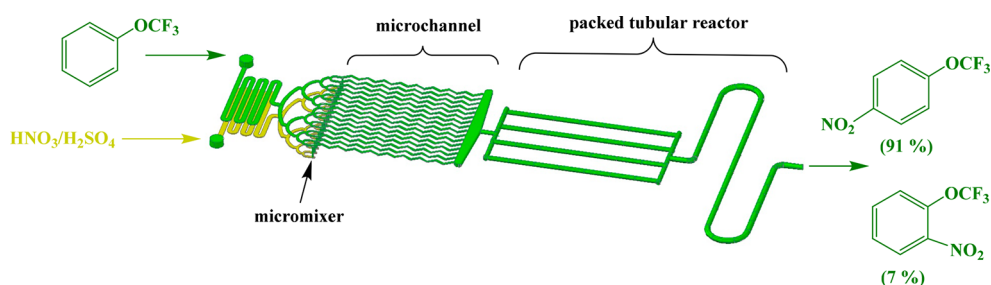

Figure 9. Schematic setup of strategy B for the scale up of the continuous flow nitration of TFMB.

Table 2. Screen of the Flow Rate on the Scale up of the Continuous Flow TFMB Nitration

entry	Q_{or} (mL·min^{-1})	Q_{aq} (mL·min^{-1})	GC (mol %)					
			TFMB	p-NB	o-NB	m-NB	DNB	conversion
1	8	20	0	91.58	6.58	0.08	1.76	100.0
2	10	24.2	0.45	91.08	7.05	0.08	1.34	99.55
3	12	29.5	2.68	88.90	6.86	0.08	1.47	97.32
4	15	36.5	8.40	83.50	6.58	0.08	1.43	91.60

with the conversion of TFMB being 99.6%. The results showed that the microreactor coupled with distributed packed tubular reactor could conduct the continuous flow nitration of TFMB well with a good performance. The precise control of temperature distribution and the efficient mixing in microreactor ensured the nitration reaction proceeded at a fast rate and minimized the formation of the byproducts compared to that in a batch system.

3. CONCLUSION

In summary, experiments were performed to study the effects of reaction parameters in the process development of the continuous flow nitration of TFMB thoroughly. The conversion and selectivity of the products were investigated by changing various parameters, including residence time, reaction temperature, sulfuric acid strength, molar ratio, flow rate, and reactor structure. The highest conversion (99.6%) of reactant was obtained in the microchannel coupled with tubular reactor system at the condition of N/S = 0.25, N/F = 1.1, φ = 97 wt %, T = 273 K, Q_{or} = 0.4 mL·min^{-1}, and Q_{aq} = 0.9 mL·min^{-1}, with the selectivity of o-NB, m-NB, p-NB, and DNB being 7.26%, 0.08%, 90.97%, and 1.04%, respectively.

Encouraged by the lab-scale results, the scale-up of the nitration of TFMB with several strategies were performed. A 0.99 kg/h throughput was achieved in the microreactor coupled with distributed packed tubal reactor system, with the selectivity of main products being 98.13% and byproducts being limited below 1.42% (0.08% of m-NB and 1.34% of DNB). The process is amenable for the preparation of analogous compounds and can easily be scaled-up by either increasing reactor size or numbering up the reactors in parallel. Further development of this procedure is currently ongoing in our laboratory.

4. EXPERIMENTAL SECTION

4.1. General. GC calibration curves were measured for trifluoromethoxybenzene (TFMB), mononitration product (p-NB, m-NB and o-NB), dinitration product (DNB), and nitrobenzene as external standard for quantitative yield calculations. For the GC assay yields, area responses were normalized with respect to nitrobenzene as the external standard and corrected for molar relative response factors. The components (retention time) observed by GC were: TFMB (4.6 min), m-NB (9.9 min), p-NB (10.2 min), o-NB (10.6 min), and DNB (14.5 min). GC analysis was performed on an Agilent 7890B with flame ionization detector using a HP1701 column (30 m × 0.32 mm × 1.0 μm), and helium was the carrier gas (1 mL·min^{-1} constant flow). After 1 min, the temperature was increased from 80 to 280 °C at a rate of 12 °C·min^{-1} and kept constant at 280 °C for 10 min. The hydrogen flow rate was 30 mL·min^{-1}; the front inlet temperature was 260 °C, and the detection temperature was 300 °C. The purity and supplier for each chemical were: trifluoromethoxybenzene (99% purity, Qi-Chem), sulfuric acid

(98 wt %, Kemiou), fuming nitric acid (98 wt %, Kemiou), sodium bicarbonate (99.5% purity, Kemiou), sodium chloride (99.5% purity, BoDi), and ethylene glycol (99.0% purity, Sinopharm).

4.2. General Laboratory Process Developmental Procedure. The general laboratory process developments were carried out in microchannel reactors. TFMB (7.57 M, flow rate of 0.4−1.0 mL·min^{-1}) and a solution of fuming nitric acid in concentrated sulfuric acid (2.49−3.19 M, flow rate of 0.8−2.2 mL·min^{-1}) were delivered by two syringe pumps (TYD01-02, Lead Fluid), respectively. The fluids reacted in capillaries with a length defined by the desired residence times and flow rates. The reaction temperature was controlled by a thermostat (F12-ME refrigerated/heating circulator, Julabo). The precooling unit, micromixer, microchannel reactor, and microneutralizer were all made up of stainless steel with an inner diameter being 0.6 mm, and immerged in the thermostat to obtain a uniform reaction temperature. At the outlet, the reaction was quenched by a large amount of water flow (10 mL·min^{-1}). The product was collected into a small beaker containing ice deionized water and separated via a separatory funnel. The organic phase was washed with saturated NaHCO$_3$ solution and deionized water for several times to remove the dissolved trace acid and inorganic substances, respectively. Then, the product was analyzed by GC. The reaction conditions were optimized by changing various parameters, including the temperature, the sulfuric acid strength, the residence time, the molar ratio of nitric acid to TFMB, flow rate, and reactor structure.

4.3. General Scale-up Process. A microreactor, consisting of four plates, 16 channels per plate with the size and total volume of microchannels being 1 mm × 0.5 mm × 85 mm and 2.72 mL, was combined with a tubular packed reactor to conduct the scale-up of continuous flow nitration. The tubular packed reactor was made up by several coilers with different length and size, and two kinds of average size of cylindrical quartz sand microparticles were used as packed particles, the average diameters of which are 2 mm and 3 mm, respectively. TFMB (7.57 M, flow rate of 10−20 mL·min^{-1}) and a solution of fuming nitric acid in concentrated sulfuric acid (3.19 M, flow rate of 24−39 mL·min^{-1}) were pumped into microreactor by two metering pumps (P1, P2, SSI, USA), respectively. The temperature of the microreactor was controlled by the microchannel heat exchanger which is integrated in the microreactor system. Then the mixed solution was introduced into the tubular packed reactor, which was put into a sink contained the cold sodium chloride solution (15%, −9 °C) to maintain the reaction temperature. At the outlet, the product was collected into product tank (3 L) containing ice deionized water and then separated via a separatory funnel. The organic phase was washed with saturated NaHCO$_3$ solution and deionized water for several times. Then 0.99 kg/h of desired product o-NB and p-NB were obtained as yellow liquid with a GC purity of 7.05% and 91.08%, while the selectivity of the

undesired product *m*-NB and DNB were limited at 0.08% and 1.34%.

ASSOCIATED CONTENT

Ⓢ Supporting Information

The Supporting Information is available free of charge on the ACS Publications website at DOI: 10.1021/acs.oprd.7b00291.

> GC spectra for compound involved in this reaction and pictures of different equipment used in the process (PDF)

AUTHOR INFORMATION

Corresponding Author

*E-mail: gwchen@dicp.ac.cn.

ORCID Ⓞ

Guangwen Chen: 0000-0001-5290-7921

Notes

The authors declare no competing financial interest.

ACKNOWLEDGMENTS

REFERENCES

(1) Rambabu, D.; Bhavani, S.; Nalivela, K. S.; Mukherjee, S.; Rao, M. B.; Pal, M. *Tetrahedron Lett.* **2013**, *54* (17), 2151−2155.

(2) (a) Ge, Z.; Hao, M.; Xu, M.; Su, Z.; Kang, Z.; Xue, L.; Zhang, C. *Eur. J. Med. Chem.* **2016**, *107*, 48−62. (b) Thompson, A. M.; O'Connor, P. D.; Blaser, A.; Yardley, V.; Maes, L.; Gupta, S.; Launay, D.; Martin, D.; Franzblau, S. G.; Wan, B.; Wang, Y.; Ma, Z.; Denny, W. A. *J. Med. Chem.* **2016**, *59* (6), 2530−2550.

(3) (a) Manteau, B.; Pazenok, S.; Vors, J.-P.; Leroux, F. R. *J. Fluorine Chem.* **2010**, *131* (2), 140−158. (b) Hojczyk, K. N.; Feng, P.; Zhan, C.; Ngai, M.-Y. *Angew. Chem., Int. Ed.* **2014**, *53* (52), 14559−14563. (c) Kirsch, P.; Bremer, M. *Angew. Chem., Int. Ed.* **2000**, *39* (23), 4216−4235.

(4) Kulkarni, A. A. *Beilstein J. Org. Chem.* **2014**, *10*, 405−24.

(5) van Woezik, B. A. A.; Westerterp, K. R. *Chem. Eng. Process.* **2002**, *41* (1), 59−77.

(6) (a) Hessel, V.; Cortese, B.; de Croon, M. H. J. M. *Chem. Eng. Sci.* **2011**, *66* (7), 1426−1448. (b) Hessel, V.; Kralisch, D.; Kockmann, N.; Noel, T.; Wang, Q. *ChemSusChem* **2013**, *6* (5), 746−789. (c) Gutmann, B.; Cantillo, D.; Kappe, C. O. *Angew. Chem., Int. Ed.* **2015**, *54* (23), 6688−6728. (d) Yao, C.; Dong, Z.; Zhao, Y.; Chen, G. *Chem. Eng. Sci.* **2015**, *123*, 137−145. (e) Gemoets, H. P. L.; Su, Y.; Shang, M.; Hessel, V.; Luque, R.; Noel, T. *Chem. Soc. Rev.* **2016**, *45* (1), 83−117. (f) Porta, R.; Benaglia, M.; Puglisi, A. *Org. Process Res. Dev.* **2016**, *20* (1), 2−25. (g) Adamo, A.; Beingessner, R. L.; Behnam, M.; Chen, J.; Jamison, T. F.; Jensen, K. F.; Monbaliu, J.-C. M.; Myerson, A. S.; Revalor, E. M.; Snead, D. R.; Stelzer, T.; Weeranoppanant, N.; Wong, S. Y.; Zhang, P. *Science* **2016**, *352* (6281), 61−67. (h) Protasova, L. N.; Bulut, M.; Ormerod, D.; Buekenhoudt, A.; Berton, J.; Stevens, C. V. *Org. Process Res. Dev.* **2013**, *17* (5), 760−791. (i) Movsisyan, M.; Delbeke, E. I. P.; Berton, J. K. E. T.; Battilocchio, C.; Ley, S. V.; Stevens, C. V. *Chem. Soc. Rev.* **2016**, *45* (18), 4892−4928. (j) Plutschack, M. B.; Pieber, B.; Gilmore, K.; Seeberger, P. H. *Chem. Rev.* **2017**, *117*, 11796.

(7) (a) Burns, J. R.; Ramshaw, C. *Chem. Eng. Commun.* **2002**, *189* (12), 1611−1628. (b) Kulkarni, A. A.; Kalyani, V. S.; Joshi, R. A.; Joshi, R. R. *Org. Process Res. Dev.* **2009**, *13* (5), 999−1002. (c) Su, Y.; Zhao, Y.; Jiao, F.; Chen, G.; Yuan, Q. *AIChE J.* **2011**, *57* (6), 1409−1418. (d) Yu, Z. Q.; Lv, Y. W.; Yu, C. M.; Su, W. K. *Org. Process Res. Dev.* **2013**, *17* (3), 438−442. (e) Shen, J. N.; Zhao, Y. C.; Chen, G. W.; Yuan, Q. *Chin. J. Chem. Eng.* **2009**, *17* (3), 412−418. (f) Chen, Y.; Zhao, Y.; Han, M.; Ye, C.; Dang, M.; Chen, G. *Green Chem.* **2013**, *15* (1), 91−94. (g) Knapkiewicz, P.; Skowerski, K.; Jaskolska, D. E.; Barbasiewicz, M.; Olszewski, T. K. *Org. Process Res. Dev.* **2012**, *16* (8), 1430−1435.

(8) Brocklehurst, C. E.; Lehmann, H.; La Vecchia, L. *Org. Process Res. Dev.* **2011**, *15* (6), 1447−1453.

(9) (a) Kockmann, N.; Gottsponer, M.; Roberge, D. M. *Chem. Eng. J.* **2011**, *167* (2−3), 718−726. (b) Kockmann, N.; Roberge, D. M. *Chem. Eng. Process.* **2011**, *50* (10), 1017−1026. (c) Elvira, K. S.; Solvas, X. C. i.; Wootton, R. C. R.; deMello, A. J. *Nat. Chem.* **2013**, *5* (11), 905−915. (d) Noel, T.; Su, Y.; Hessel, V. Beyond Organometallic Flow Chemistry: The Principles Behind the Use of Continuous-Flow Reactors for Synthesis. In *Topics in Organometallic Chemistry*; Noel, T., Ed.; Springer, 2015; Vol. 57, pp 1−41.10.1007/3418_2015_152 (e) Zhang, J.; Wang, K.; Teixeira, A. R.; Jensen, K. F.; Luo, G. *Annu. Rev. Chem. Biomol. Eng.* **2017**, *8*, 285.

(10) Gage, J. R.; Guo, X.; Tao, J.; Zheng, C. *Org. Process Res. Dev.* **2012**, *16* (5), 930−933.

(11) Kapustin, E. G.; Bzhezovsky, V. M.; Yagupolskii, L. M. *J. Fluorine Chem.* **2002**, *113* (2), 227−237.

(12) Shirejini, S. Z.; Mohammadi, A. *Org. Process Res. Dev.* **2017**, *21* (3), 292−303.

(13) Sharma, Y.; Joshi, R. A.; Kulkarni, A. A. *Org. Process Res. Dev.* **2015**, *19* (9), 1138−1147.

(14) Ravikumar Bandaru, S. V.; Ghosh, P. *Int. J. Heat Mass Transfer* **2011**, *54* (11−12), 2245−2252.

(15) (a) Zhao, Y.; Chen, G.; Yuan, Q. *AIChE J.* **2007**, *53* (12), 3042−3053. (b) Tang, J.; Zhang, X.; Cai, W.; Wang, F. *Exp. Therm. Fluid Sci.* **2013**, *49*, 185−192. (c) Antony, R.; Nandagopal, M. S. G.; Sreekumar, N.; Rangabhashiyam, S.; Selvaraju, N. *Bull. Chem. React. Eng. Catal.* **2014**, *9* (3), 207−223.

(16) Su, Y.; Zhao, Y.; Chen, G.; Yuan, Q. *Chem. Eng. Sci.* **2010**, *65* (13), 3947−3956.